Journal of

Applied and Computational Mechanics

Shahid Chamran
University of Ahvaz

Journal of Applied and Computational Mechanics

Mathematical Analysis of Poiseuille Flow of Casson Fluid past Porous Medium

D.S. Sankar[1] , K.K. Viswanathan[2,3]

[1] School of Applied Sciences and Mathematics, Universiti Teknologi Brunei
Jalan Tungku Link, Gadong, BE1410, Bandar Seri Begawan, Brunei Darussalam, Email: duraisamy.sankar@utb.edu.bn

[2] Ship & Offshore Extreme Technology Industry-Academic Cooperation Research Center, Department of Naval Architecture and Ocean Engineering, Inha University
100 Inha-ro, Michulol-gu, Incheon 22212, Republic of Korea, Email: visu20@yahoo.com

[3] Department of Mathematics, Academy of Maritime Education and Training (AMET) (Deemed to be University), 135, East Coast Road, Kanathur, Chennai-603 112, India

Abstract. In this article, the influence of microstructure in the Casson fluid flow through a porous medium is investigated, by extending the Buckingham-Reiner's one-dimensional model to plane-Poiseuille flow and Hagen-Poiseuille flow geometries. While analyzing the flow characteristics in single-channel/pipes or multiple channels/pipes of different width/radius, four different probability density functions are used to model the pores widths/radii distributions. It is found that when the pressure gradient increases, the Buckingham-Reiner function raises slowly in the plane-Poiseuille flow, whereas in Hagen-Poiseuille flow, it rises rapidly. In all kinds of distribution of pores, the fluid's mean velocity and porosity of the flow medium are considerably higher in the Hagen-Poiseuille flow than in the plane-Poiseuille flow, and this behavior is reversed for the permeability of the flow medium. The fluid's mean velocity, porosity, and permeability of the flow medium increases appreciably with the rise of the channel width and pipe radius. The porosity of the flow medium slumps with the rise of the period H of the channels and pipes distribution from 1 to 2, and it decreases very slowly with the further rise of the period H of the channels and pipes from 2 to 11.

Keywords: Poiseuille flow in channel/pipe; Casson fluid; Mean velocity; Porous medium; Permeability; Pores distribution.

1. Introduction

Several materials which we use in our everyday life, for example, toothpaste, emulsions, whipped cream, varnish, gels, syrups, edible oils, etc., cannot be classified into either elastic solids or simple fluids, are classified as non-Newtonian fluids [1, 2]. Among the several non-Newtonian fluids, indeed, some of them exhibit the yield threshold (yield stress), meaning that it is the stress level below which the fluid moves like a solid (which is termed as plug flow) and if the stress level exceeds this threshold limit, the fluid undergoes normal shear flow [3, 4]. Some examples of the well-known non-Newtonian fluids are semi-solid foods, paints, slurries, sauce, ketchup, corn starch, mud, drilling fluids, crude oil, etc. Herschel-Bulkley (H-B) fluid, Casson fluid, and Bingham fluid are some of the yield stress fluids which finds applications in many fields of bio-sciences, bio-medical engineering, petroleum, and chemical engineering, food industries, etc. [5 – 10].

Bingham fluid model is a non-Newtonian fluid with yield stress which has a linear relationship between the stress and rate of strain and, its yield stress is a stress level beyond which the fluid exhibits Newtonian fluid's flow behavior [11]. H-B fluid is a yield stress fluid model that has three fluid parameters, such as power-law index, viscosity coefficient, and yield stress. This fluid model can describe the behavior of power-law fluid (shear thinning or shear thickening behavior) at zero yield stress, and it exhibits the Bingham fluid's flow behavior when the power-law index n = 1 and Newtonian fluid model when the yield stress τ_y = 0 and power-law index n = 1 [12,13]. Casson fluid model is also an important non-Newtonian fluid model that has two rheological parameters such as coefficient of viscosity and yield stress. It reduces to Newtonian fluid model when the yield stress τ_y = 0 [14]. Since the Casson fluid's constitutive equation is a nonlinear empirical relation between the stress and strain rate which can be used to model many fluid flow problems that are inherently nonlinear and the resulting mathematical model can be solved using either analytical method or computational methods without making any conceptual approximation (linearization) in the governing equations, it is used to model the present fluid flow problem [15, 16].

A porous media is a material composed of the network of pores, and it is often encountered as the flow medium, which has the vital characteristics such as porosity, permeability, tensile strength, electrical conductivity, tortuosity, etc. [17, 18]. The rheology of non-Newtonian fluids through porous medium finds applications in several fields such as observing nutrients from digestive system for distribution in the bloodstream, blood propagation through the kidney, the observation of rainwater by earth's surface, removal of pollutants from effluent water in the treatment plant, injection of drilling fluids in rocks for strengthening of oil well and enhancing oil recovery, glue penetration in the porous surface of solid materials, injection of cement grouts, slurries or muds to improve soil strength [19 – 21].
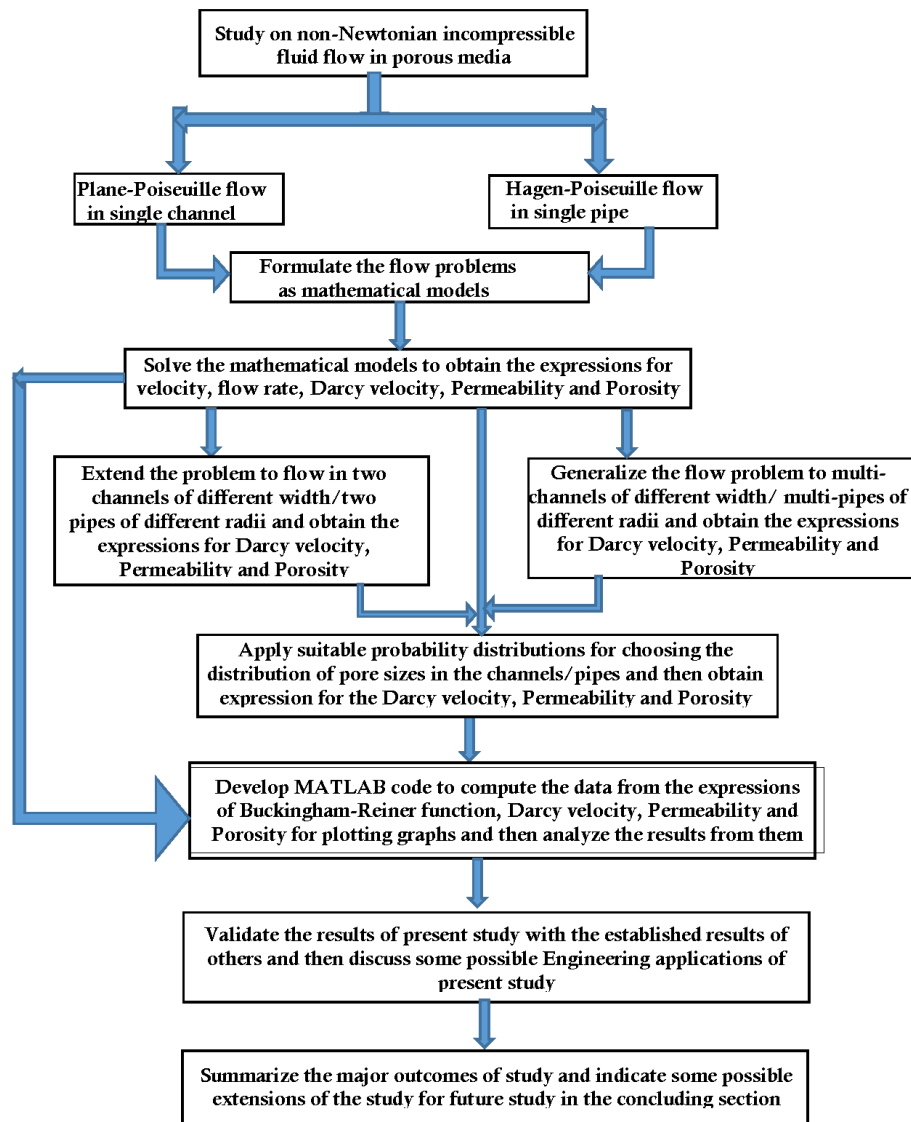
Fig. 1. Schematic configuration of the flow system under study.

The seminal contribution of Darcy [22] to the field of fluid flow in porous media attracted several researchers to advance the research in this field for different rheological geometries and physical conditions. Among the pores that form a network of the porous medium, the percolating conduits are the prime part of the porous medium as they observe the significant amount of fluids compared to the pores that are discretely distributed either at the end or at the other parts of the flow medium [23]. Computation of the size of the pore with these percolating conditions is a great challenge in the fluid flow problems [24]. Several researchers developed various techniques to find the characteristics of porous size distribution in the flow medium [25, 26]. Mercury intrusion porosimetry is one of these techniques which involve the injection of mercury into the porous medium and is based on the presence of a threshold below which the pores cannot be intruded by the fluid [27]. The BJH method (Barret, Joyner, and Halenda) is another method of finding the pore size distribution which makes use of the mechanisms of isothermal adsorption by the pore walls and the condensation by capillary which is owing to the molecular Van der Waals interactions between the condensing vapor and the internal surface of the pores [28].

Buckingham [29] and Reiner [30] obtained the formula for finding the rate of fluid flow in a cylindrical pipe which is named as Buckingham-Reiner law. Several researchers studied this problem for different types of flow geometries and various other aspects of this flow [31, 32]. Dapra and Scarpi [33] investigated the unsteady flow through the plane channel and used the Pascal model to obtain the series solution for the start-up flow and later [34], they extended this study to flow through the cylindrical pipe. Chen et al. [21] investigated the one-dimensional flow within the framework of the two-dimensional network. Balhoff et al. [18] propounded effective numerical methods for estimating the rheological measures of the fluid flow through porous networks. Chevalier and Talon [35] analyzed the flow in a diamond-shaped porous network, and they assigned a random threshold to different paths. Chevaliar et al. [36] experimentally obtained the appropriate Darcy law for the Herschel-Bulkley flow through a porous medium and pointed out the non-Newtonian characteristics of the flowing fluid. Bleyer and Coussot [19] numerically modeled the flow of Bingham fluid through an array of circular tubes. Nash and Rees [37] investigated the effects of pores in the one-dimensional Bingham fluid flow through a channel and pipe, assuming that the pores in the channel/pipes are distributed in some types of probability density functions. The present mathematical analysis attempts to study the influence of pressure gradient, width of channel/pipe radius, period of channels/pipes distribution on the mean velocity, porosity and permeability of the flow medium in the (i) plane-Poiseuille flow and (ii) Hagen-Poiseuille flow of Casson fluid through single channel/single pipe and multi-channel/multi-pipes. Three types of probability density functions, such as uniform distribution, quadratic distribution, and two forms of linear distribution, are used to model the distribution of the pores in the porous flow medium. The meaning/importance of the present study from the physics perspective is explained below with some typical examples:
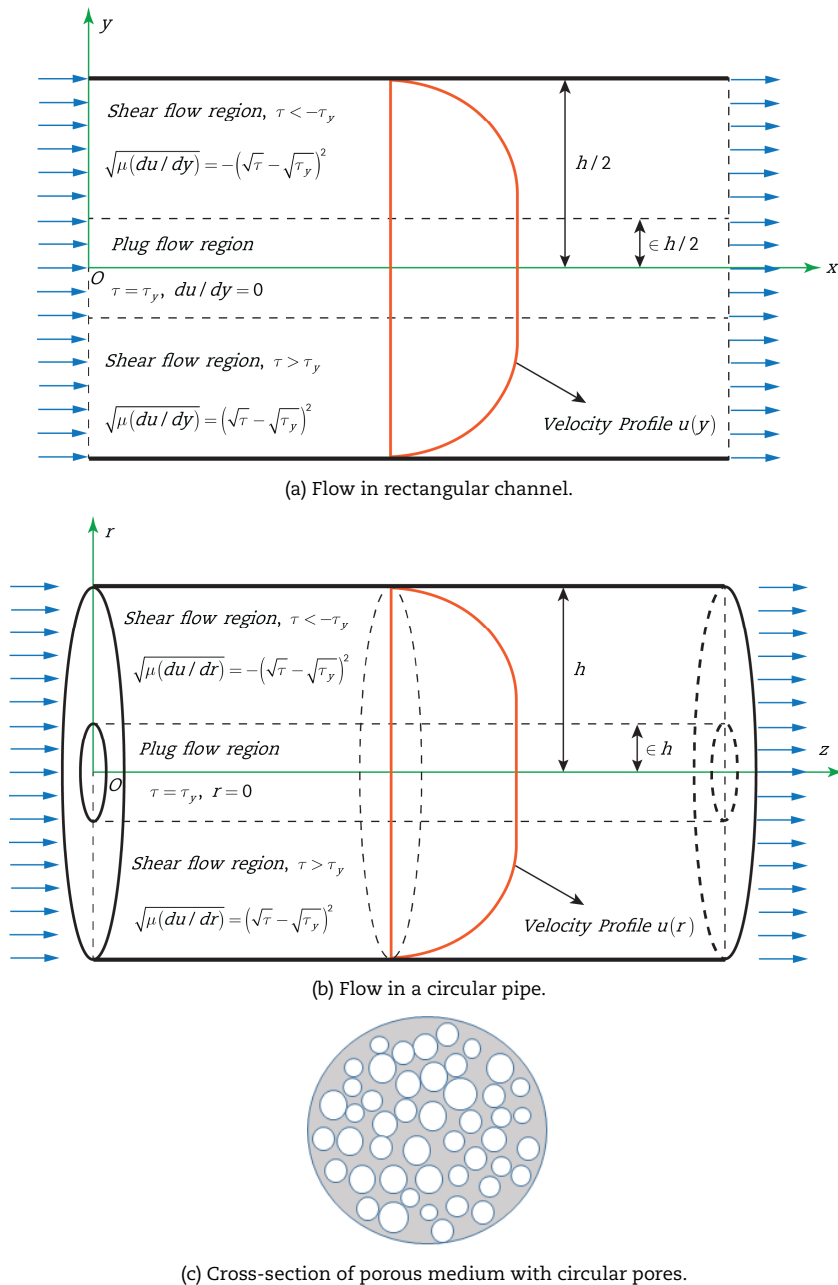
(a) Flow in rectangular channel.

(b) Flow in a circular pipe.

(c) Cross-section of porous medium with circular pores.

Fig. 2. Flow geometry in a porous medium.

The non-Newtonian fluids flow in porous media is an important physical phenomenon that has several potential applications such as blood flow in capillaries and tissues, injection of drilling fluids in the mining industry to strengthen the walls of mines, the flow of viscoplastic and Newtonian fluids through argillaceous soils, etc.. [20]. Some of the injecting fluids which are used in the oil industry show the strong characters of non-Newtonian fluids with yield stress that move like liquid only if the applied stress is larger than a critical value (yield stress) [21, 38, 39]. The flow of such non-Newtonian fluids in a porous medium is noted with the strong characteristics of yield stress, which likely induces specific fluid properties that are so not investigated in depth so far. Though Bingham fluid and Casson fluid are non-Newtonian fluid models with a yield stress, the constitutive equation Casson fluid models is highly nonlinear compared to that of Bingham fluid. Thus the Casson fluid model can exhibit more complex behavior of nonlinear fluids when they flow past a porous medium consisting of a bundle of channels of different width/ pipes of different radii. The present study not only analyses the effects of pressure gradient on the Buckingham-Reiner function and Darcy mean velocity but also discusses in depth the influence of the width of channels/radii of pipes, period of channels/pipes in the porous medium/network of permeability of the flow medium. Moreover, this paper points out that the porosity and permeability of the fluid flow in the porous medium have the same characteristic in all types of distribution of channels widths/pipes radii that are defined by the three different types of probability density functions.

The organization of this research article is given below in brief:

Section 2 formulates the fluid flow problem mathematically and then the analytical solutions for the rheological quantities, viz. velocity profile, flow rate, Buckingham-Reiner formula, mean velocity in single channel/single pipe, mean velocity in multi-channel/multi-pipe, porosity, and permeability in plane-Poiseuille and Hagen-Poiseuille flows are also obtained in this section. The influence of the flow parameters such as pressure gradient, the width of channel/radius of the pipe, the period of rectangular channel/cylindrical pipes distribution in the flow medium on the important rheological quantities such as Buckingham – Reiner function, mean velocity, porosity and permeability of the flow medium are analyzed in Section 3 through the appropriate graphical representation of data computed from these functions. The major results of this study are collated in the conclusion section 4. The flow chart for the schematic configuration of the flow system under study is given in Fig. 1.

2. Mathematical Framework

2.1 Plane-Poiseuille flow in single-channel

Let us consider the axisymmetric, plane Poiseuille flow of viscous incompressible fluid in a rectangular channel of width h bounded by the planes $y = \pm h/2$. The geometries of the fluid flow in a rectangular channel and circular pipe are shown in Fig. 2(a) and 2(b) respectively. The cross-sectional geometry of the porous medium with circular pores is depicted in Fig. 2(c) (The rheological measures pertaining to the Hagen-Poiseuille flow are obtained in Appendix).

Let $u(=u(y))$ be the fluid velocity along the x axis. Since the flow considered here is uni-directional and isothermal, the simplified form of the momentum equation governing this flow is:

$$-\frac{dp}{dx} + \frac{d\tau}{dy} = 0, \tag{1}$$

where $\tau(=\tau_{xy})$ and p are the shear stress and fluid pressure, respectively.

The flowing incompressible fluid is modeled as a Casson fluid model whose constitutive equation (empirical relation connecting the shear stress and rate of strain) for its flow in the channel is given as under:

$$\sqrt{\mu\frac{du}{dy}} = \left(\sqrt{\tau} - \sqrt{\tau_y}\right) \text{ if } \tau > \tau_y, \tag{2}$$

$$\frac{du}{dy} = 0 \text{ if } -\tau_y < \tau < \tau_y, \tag{3}$$

$$\sqrt{\mu\frac{du}{dy}} = -\left(\sqrt{\tau} - \sqrt{\tau_y}\right) \text{ if } \tau < -\tau_y, \tag{4}$$

where μ is the Casson fluid's viscosity coefficient. The boundary conditions that are appropriate to this flow are

$$\tau = 0 \text{ at } y = 0; \quad u = 0 \text{ at } r = \pm h/2 \tag{5}$$

For computational convenience, let us denote the pressure drop per unit length as $G(=-dp/dx)$ which is a positive quantity that makes the fluid velocity to be positive as it is non-zero. Solving Eq. (1) along with the boundary condition (5a), we obtain the simplified expression for the shear stress as $\tau = Gy$. Since the Casson fluid has non-zero yield threshold, the flow domain in the channel is divided into three regions as described below:

Part –I: $\quad -\frac{h}{2} \leq y \leq -\frac{\in h}{2}$ (Lower part – Shear flow region).

Part – II: $\quad -\frac{\in h}{2} \leq y \leq \frac{\in h}{2}$ (Middle part – Plug flow region).

Part – III: $\quad \frac{\in h}{2} \leq y \leq \frac{h}{2}$ (Upper part – Shear flow region).

Since the flow considered is axisymmetric, the fluid's velocity in the upper region (part III) and lower region (part I) of the flow regions are equal, and thus, it is enough to find the expression for velocity in the upper part of the shear flow region and in the plug-flow region. From Eqs. (4) and (5b), one can obtain the velocity of Casson fluid in the upper region (Part III) and plug flow (solid-like flow) region (Part II) as below respectively:

$$u(y) = \frac{\Omega}{8\mu}\left(h^2 - 4y^2\right) + \frac{\tau_y}{\mu}\left(\frac{h}{2} - y\right) - \frac{\sqrt{2\Omega\tau_y}}{3\mu}\left(h^{3/2} - 2\sqrt{2}y^{3/2}\right) \text{ if } \frac{\in h}{2} \leq y \leq \frac{h}{2}, \tag{6}$$

$$u_P = \frac{\Omega h^2}{8\mu}\left(1 - \in^2\right) + \frac{\tau_y h}{2\mu}\left(1 - \in\right) - \frac{\sqrt{2\Omega\tau_y h^3}}{3\mu}\left(1 - \in^{3/2}\right) \text{ if } -\frac{\in h}{2} \leq y \leq \frac{\in h}{2}, \tag{7}$$

where $\in = 2\tau_y/\Omega h$ is the proportion of the channel where plug flow occurs, Ω is the pressure gradient and the expression for the velocity profile in Eq. (6) is valid only when $\in < 1$. If $\in > 1$, then the plug flow would happen in the whole channel region. Let $\sigma = 1/\in = \Omega h/2\tau_y$, then, σ is the dimensionless pressure gradient which mainly depends on the fluid's yield stress. It is realized that the fluid starts to flow when σ increases above unity and thus $\sigma = 1$ is the threshold level of pressure gradient.

Since our objective is to study the flow through a porous medium, we assume that the porous flow medium comprises of a periodic array of channels/pipes of the period H. Then, the flow medium's porosity is $\phi = h/H$. The total flow rate Q within one channel is obtained as below:

$$Q = \int_{-h/2}^{h/2} u\,dy = 2\left[\int_0^{\in h/2} u_{pl}\,dy + \int_{\in h/2}^{h/2} u\,dy\right] = \frac{\Omega h^3}{12\mu}f(\sigma) = \frac{\Omega h^2}{6\mu}\sigma f(\sigma), \tag{8}$$

where

$$f(\sigma) = \begin{cases} 1 - \dfrac{12}{5\sqrt{|\sigma|}} + \dfrac{3}{2|\sigma|} - \dfrac{1}{10|\sigma|^3} & \text{if } |\sigma| > 1 \\ 0 & \text{otherwise} \end{cases}. \tag{9}$$

The function $f(\sigma)$ obtained in Eq. (9) is the Buckingham- Reiner function (formula) for the plane-Poiseuille rheology of Casson fluid. When the yield stress $\tau_y = 0$ (i.e. $\in = 1/\sigma = 0$), Casson fluid model deduces to Newtonian fluid model. It is noted that when $\in = 0$ (Casson fluid model reduces to Newtonian fluid model), the expressions obtained for the flow rate in Eqs. (8) and (A1) (in the Appendix) for the plane-Poiseuille flow and Hagen-Poiseuille flow respectively are in good agreement with the expression obtained by Nash and Rees [36] in their Eqs. (6) and (48) respectively (Bingham fluid model reduced to Newtonian fluid model when $\in = 0$). Since we restrict the pressure gradient Ω as positive, σ would be positive and henceforth we use σ rather than $|\sigma|$. The Darcy velocity of Casson fluid u_C is its mean velocity which is computed over a period of the channels' pattern as below:

$$u_C = \frac{\phi\Omega h^2}{12\mu}f(\sigma) = \frac{\Omega K}{\mu}f(\sigma), \tag{10}$$

where

$$\phi = \frac{h}{H} \text{ and } K = \frac{\phi h^2}{12}, \tag{11}$$

are the porosity and permeability of the porous medium, respectively. These are some of the prime parameters of this study, which strongly depends on the channels' choice and are used to find the period of a porous medium. An important criterion for this flow is that $\sigma >> 1$, and thus, one can easily obtain the mean velocity of Newtonian fluid flow as $u_N = \Omega K / \mu$. The normalized mean velocity $f(\sigma)$ of the Casson fluid (comparing the response of Casson fluid and Newtonian fluid for flow in a channel) in plane-Poiseuille flow is defined as:

$$f(\sigma) = u_C / u_N \tag{12}$$

From Eq. (9), we note that $f(\sigma) \to 1$ as $\sigma \to \infty$. The normalized mean velocity $f(\sigma)$ close to threshold values reduce to the quadratic form as below:

$$f(\sigma) = \frac{1}{4}(\sigma - 1)^3 - \frac{21}{32}(\sigma - 1)^4 + \dots, \quad 0 < (\sigma - 1) << 1 \tag{13}$$

For an extremely higher value of σ, Casson fluid exhibits Newtonian fluid's behavior. The three-term approximation to the induced flow $\sigma f(\sigma)$ can be obtained as:

$$\sigma f(\sigma) \approx \sigma - \frac{12}{5}\sqrt{\sigma} + \frac{3}{2}, \qquad \sigma >> 1 \tag{14}$$

The equivalent flow quantities for the Hagen-Poiseuille flow (flow in a circular pipe) of Casson fluid are obtained in the Appendix, where $g(\sigma)$ is the normalized mean velocity of Casson fluid in the circular tube of radius h. Henceforth, we use the notation $F(\sigma)(= u_C / u_N)$ and $G(\sigma)(= u_C / u_N)$ to represent the ratio formed between the volume flow rate of Casson fluid and that of Newtonian fluid in channel and tube flow respectively.

2.2 Effect of two channels of different width

The rectangular/circular shape of pores in the porous flow medium are the more widely encountered/adopted pore shapes in nature and industrial applications. For some specific purposes, we design the porous medium with other kinds of pore shapes, such as triangle, pentagonal, hexagonal, etc. In this study, we consider that the porous medium with rectangular and circular pores [40]. Firstly, we consider the porous medium that has one period of channels, which consists of the first channel of width h and a second narrower channel of width γh where $\gamma < 1$. The total flux of Casson fluid flow through one period of channels (with a broader channel of width h and a narrow channel of width γh) is given by the formula [Nash and Rees, 37]:

$$Q = \Omega h^3 \left[f(\sigma) + \gamma^3 f(\gamma\sigma) \right] / 12\mu. \tag{15}$$

The Darcy velocity for this flow is:

$$u_B = (\Omega K / \mu) \left[f(\sigma) + \gamma^3 f(\gamma\sigma) \right] / (1 + \gamma^3). \tag{16}$$

The mean velocity of Casson fluid relative to that of Newtonian fluid is:

$$u_B / u_N = F(\sigma) = \left[f(\sigma) + \gamma^3 f(\gamma\sigma) \right] / (1 + \gamma^3). \tag{17}$$

The porosity and permeability of the channel medium are obtained respectively as:

$$\phi = h(1 + \gamma) / H, \tag{18}$$

$$K = (\phi h^2 / 12) \left[(1 + \gamma^3) / (1 + \gamma) \right]. \tag{19}$$

2.3 Effect of multi-channels of different width

Now, we generalize the two-channel per period of the porous medium to N channels per period of the porous flow medium. Let us assume the width of the channels as $\gamma_i h$ for $i = 1, 2, ..., N$, and the channels are put in the descending order of their width, then we have:

$$1 = \gamma_1 \geq \gamma_2 \geq .... \gamma_N. \tag{20}$$

The Darcy velocity of Casson fluid through N channels per period of the porous medium is defined by:

$$u_C = (\Omega K/\mu) \left[\sum_{i=1}^{N} \gamma_i^3 f(\gamma_i \sigma) \Big/ \sum_{i=1}^{N} \gamma_i^3 \right]. \tag{21}$$

The Darcy mean velocity of Casson fluid relative to that of Newtonian fluid is defined as:

$$u_C / u_N = F(\sigma) = \left[\sum_{i=1}^{N} \gamma_i^3 f(\gamma_i \sigma) \Big/ \sum_{i=1}^{N} \gamma_i^3 \right]. \tag{22}$$

The porosity and permeability of the porous medium, which has N channels per period are respectively given below:

$$h = (h/H) \sum_{i=1}^{N} \gamma_i \tag{23}$$

$$K = \left(\phi h^2 / 12 \right) \left[\sum_{i=1}^{N} \gamma_i^3 \Big/ \sum_{i=1}^{N} \gamma_i \right]. \tag{24}$$

For the Hagen-Poiseuille fluid flow in a porous medium, which comprise of multi-circular tubes, the expressions similar to Eqs. (20) – (24) are obtained in the Appendix.

2.4 Channels' random distribution

The distribution of pores in the flow medium mostly has some particular pattern which often follow some particular probability distributions. In this study, to analyze the flow field, the distribution of width of the channels in the porous medium is assumed to follow the probability distributions such as (i) Uniform distribution, (ii) Linear distributions (Type I and Type II) and (iii) Quadratic distribution. Let $\psi(\gamma)$ be the probability density function of the widths of the channels in the porous medium. For fluid flow in channel, the expression for the Darcy velocity of Casson fluid relative to that of the Newtonian fluid, the porosity, and permeability of the flow medium can be obtained by using Eqs. (25) – (27) respectively [37]:

$$F(\sigma) = \int_0^\infty \gamma^3 \psi(\gamma) f(\gamma \sigma) d\gamma \Big/ \int_0^\infty \gamma^3 \psi(\gamma) d\gamma, \tag{25}$$

$$\phi = (h/H) \int_0^\infty \gamma \psi(\gamma) d\gamma, \tag{26}$$

$$F(\sigma) = \left(\phi h^2 / 12 \right) \int_0^\infty \gamma^3 \psi(\gamma) d\gamma \Big/ \int_0^\infty \gamma \psi(\gamma) d\gamma, \tag{27}$$

2.4.1 Uniform distribution

When the pores of the flow medium are uniformly distributed, its probability density function is:

$$\psi(\gamma) = \begin{cases} \dfrac{1}{1-a} & \text{if } a < \gamma < 1 \\ 0 & \text{otherwise} \end{cases}. \tag{28}$$

The Darcy velocity of Casson fluid in the multi-channel with uniformly distributed pores is:

$$F(\sigma) = \begin{cases} 0 & \text{if } 0 \leq \sigma < 1 \\ \dfrac{35\sigma^4 - 96\sigma^{7/2} + 70\sigma^3 - 14\sigma + 5}{35\sigma^4 (1 - a^4)} & \text{if } 1 \leq \sigma \leq 1/a \\ 1 - \dfrac{96(1 - a^{7/2})}{35\sqrt{\sigma}(1 - a^4)} + \dfrac{2(1 + a + a^2)}{\sigma(1+a)(1+a^2)} - \dfrac{2}{5\sigma^3 (1+a)(1+a^2)} & \text{if } \sigma > \dfrac{1}{a} \end{cases} \tag{29}$$

From Eq. (29), it is noted that depending on the range of the values of σ, the whole region of flow is divided into three regions/phases. In the first region $(0 \leq \sigma < 1)$, the flow is stagnant, while in the intermediate region $(1 \leq \sigma \leq 1/a)$, the flow develops in the proportion of channels whose width varies from h/σ to h. In the last regime $(\sigma > 1/a)$, the flow occurs in all the channels. For the present flow (channel with uniformly distributed pores), the porosity and permeability are obtained as:

$$\phi = \left(\frac{h}{H}\right)\frac{(1+a)}{2},$$ (30)

$$K = \left(\frac{\phi h^2}{12}\right)\frac{(1+a^2)}{2}.$$ (31)

When $a = 0$ (the channel width do not have a lower limit), then the third region no longer exists. Thus, we have the simplified expression for Darcy velocity as below:

$$F(\sigma) = \begin{cases} 0 & \text{if } 0 \le \sigma \le 1 \\ \dfrac{35\sigma^4 - 96\sigma^{7/2} + 70\sigma^3 - 14\sigma + 5}{35\sigma^4} & \text{if } \sigma > 1 \end{cases}$$ (32)

2.4.2 Linear distribution

Let us apply the following probability density functions of two linear distributions to describe the pattern of the pores in the flow medium:

$$(\mathrm{i}) \quad \psi(\gamma) = 2\gamma, 0 \le \gamma \le 1;$$ (33)

$$(\mathrm{ii}) \quad \psi(\gamma) = 2(1-\gamma), 0 \le \gamma \le 1;$$ (34)

For the first linear distribution (defined in Eq. (33)), the expressions for Darcy velocity, porosity, and permeability are obtained as Eqs. (35) – (37).

$$F(\sigma) = \begin{cases} 0 & \text{if } 0 \le \sigma \le 1 \\ \dfrac{25\sigma^5 - 64\sigma^{9/2} + 45\sigma^4 - 12\sigma + 21}{150\sigma^5} & \text{if } \sigma > 1 \end{cases}$$ (35)

$$\phi = \frac{2h}{3H},$$ (36)

$$K = \frac{3}{5}\left(\frac{\phi h^2}{12}\right).$$ (37)

For the second linear distribution (given in Eq. (34)), the expressions of Darcy velocity, porosity, and permeability simplify to Eqs. (38) – (40).

$$F(\sigma) = \begin{cases} 0 & \text{if } 0 \le \sigma \le 1 \\ \dfrac{126\sigma^5 - 48\sigma^{9/2} + 315\sigma^4 - 126\sigma^2 - 1422\sigma + 1155}{126\sigma^5} & \text{if } \sigma > 1 \end{cases}$$ (38)

$$\phi = \frac{h}{3H},$$ (39)

$$K = \frac{3}{20}\left(\frac{\phi h^2}{12}\right).$$ (40)

2.4.3 Quadratic distribution

The probability density functions of quadratic distributions is defined as below in Eq. (41):

$$\psi(\gamma) = 3(1-\gamma)^2, 0 \le \gamma \le 1;$$ (41)

On using the quadratic distribution to represent the width of the pores in the flow medium, one can obtain the expressions for Darcy velocity, porosity, and permeability as Eqs. (42) – (44), respectively:

$$F(\sigma) = \begin{cases} 0 & \text{if } 0 \le \sigma \le 1 \\ \dfrac{77\sigma^6 - 12928\sigma^{11/2} + 231\sigma^5 - 616\sigma^3 + 1237\sigma^2 - 385\sigma + 476}{77\sigma^6} & \text{if } \sigma > 1 \end{cases}$$ (42)

$$\phi = \frac{h}{4H},$$ (43)

$$K = \frac{1}{5}\left(\frac{\phi h^2}{12}\right).$$ (44)

2.4.4 Justification for the choice of probability density functions and their coefficients

In several industrial and real-world applications, the porous medium in fluid flow is mostly formed with channels/pipes whose widths/radii are distributed either randomly or in some particular pattern. Oukhlef [23] pointed out that the pores size distribution in the porous medium/network (which composed of channels/pipes) can be determined from the analytical solution of integral equation, which is resulted from the equation of total flux of fluid flow and the constitutive equation of flowing fluid. Through the theoretical studies, Oukhlef [23] confirmed that the pores size distribution of channels/pipes in the porous medium obtained through the aforesaid analytical solution are in good agreement with the corresponding values obtained from the normal distribution's probability density function (PDF) (refer Fig. 5 in Ref. [23]). Oukhlef [23] also propounded that the computation of pore size distribution from the PDF is quite easier than obtaining these values by solving the Volterra integral equation to obtain the analytical solution and then computing pore size distribution values from this analytical solution. Thus, for computational efficiency of pores size (width of channels/radii of pipes) distribution in the channels/pipes in porous medium/network, we use the different PDFs such as (i) uniform distribution, (ii) two types of linear distributions and (iii) quadratic distributions. It is hoped that these three types of PDFs would cover the different sizes and pattern of pores distribution (channels width/pipes radius) in the porous medium of fluid flow which we encounter in various applications of porous medium such as filtration of toxic wastages in effluent treatments plants, the absorbance of salts in the purification processes of mineral water, absorbing of bio-fluids in biological tissues, diffusion of drugs in the circulatory systems of body, water absorbance by various types of river bed, etc.

The parameter a in the PDF of uniform distribution is assigned different values in the interval to study the effect of different sizes of pores (channels widths/ pipes radii) on the mean velocity, permeability, and porosity in the fluid flow. Since the PDF of Type I of linear distribution (Eq. (33)) is monotonically increasing with γ (channels widths/pipes radii increasing with γ) and the PDF of Type II of linear distribution (Eq. (34)) is monotonically decreasing with γ in $(0,1)$ (channels widths/pipes radii decreasing with γ), we have taken '2' as their sample scaling factor to magnify (enlarge) the channels widths/pipes radii in the porous medium/network. Similarly, as the PDF of quadratic distribution (Eq. (41)) is monotonically decreasing with γ in $(0,1)$ (channels widths/pipes radii decreasing with γ), the scaling factor '3' in its PDF magnifies (enlarges) the channels widths/pipes radius as narrow.

3. Numerical Simulation of Results and Discussion

The aim of this mathematical analysis is to investigate the influence of the flow parameters, viz. pressure gradient σ, the width h of rectangular channel/radius h of a cylindrical pipe, the period H of rectangular channel/cylindrical pipes distribution in the flow medium on the important rheological metrics such as Buckingham – Reiner function $f(\sigma)$(or $g(\sigma)$), mean velocity u_C/u_N, porosity ϕ and permeability K of the flow medium, in the uni-directional flow of Casson fluid through a rectangular channel of width h/cylindrical pipe of radius h having the characteristics of porosity and permeability. The parameters used in this analysis and their range are listed hereunder [37]:

Pressure gradient $\sigma : 1-5$; Channel width / Pipe radius $h : 0.7 - 1.0$; Period of channels / pipes distribution $H : 1-11$; Ratio between the multi-Channels widths / ratio between the multi-pipes radius $\gamma : 0.5-1$; Parameter of uniform distribution $a : 0-1$ [37]. The justification for the choice of parameter range is briefed below:

The range of the pressure gradient parameter σ is taken as $1-6$ since no shear flow happens when $\sigma < 1$ (the whole flow region is unyielded when $\sigma < 1$), and as the flow under study is slow (viscous flow as the inertial terms in the momentum equations are neglected) the upper limit of the pressure gradient is limited to 6. To cover the wide range of multi-channels width/multi-pipes radius, the ranges of the single-channel width/single-pipes radius parameter h and multi-channels widths/multi-pipes radii ratio parameter γ are taken as $0.7 - 1.0$ and $0.5 - 1$ respectively [37]. To analyze the influence of different patterns of the distribution of channels/pipes on the permeability and porosity of the porous medium, the period of channels parameter H is taken in the range $1 - 11$ [37]. Similarly, to investigate the variations in the permeability and porosity of the porous medium for different choices of uniformly distributed channels width/pipes radii, its parameter a values range $(0,1)$ is adopted from Nash and Rees [37]. Some of the natural and industrial applications of these kinds of flow covering the range as mentioned earlier of parameter values are injection of cement in soils, penetration of glue in porous substances, polymer processing in packed beds and injection molding, etc. [18, 20].

It is to be noted here that in the plots of all the graphs presented in this section, dotted red lines denote the flow characteristics in Hagen-Poiseuille flow, while the continuous blue lines refer to the flow quantities' variation in plane-Poiseuille flow.

3.1 Buckingham-Reiner function

Fig. 3 depicts the variation of Buckingham-Reiner function $f(\sigma)$(or $g(\sigma)$) (normalized flow rate) with pressure gradient for the plane-Poiseuille flow (steady flow in a rectangular channel) and Hagen-Poiseuille flow (steady flow in a cylindrical tube) of Casson fluid in the porous flow medium. Firstly, we note that in the plane-Poiseuille flow of Casson fluid, the Buckingham-Reiner function increases slowly (linearly) with the pressure gradient σ, whereas in the case of Hagen-Poiseuille flow of Casson fluid, it soars up with the rise of the pressure gradient from 1 to 2.5 and then it increases very slowly (almost constant) when the pressure gradient raises from 2.5 to 5. At a given pressure gradient level, the Buckingham-Reiner function has markedly higher value in the Hagen-Poiseuille flow than in plane-Poiseuille flow.

For comparing the characteristics of Casson fluid with Bingham fluid, the variation of Buckingham-Reiner function with the pressure gradient for the plane-Poiseuille flow and Hagen-Poiseuille fluid of Bingham fluid are also sketched in Fig. 3. It is noticed that the Buckingham-Reiner function of the Hagen-Poiseuille flow is marginally higher for Casson fluid than for the Bingham fluid when the pressure gradient σ varies in the range $1 - 4.25$ and this behavior is reversed when the pressure gradient exceeds 4.25. However, in the plane-Poiseuille flow, the Buckingham-Reiner function is significantly higher for Bingham fluid than for the Casson fluid. The reasons for the aforesaid abnormal behavior of Casson and Bingham fluids between the plane-Poiseuille flow and Hagen-Poiseuille flow are explained as below:
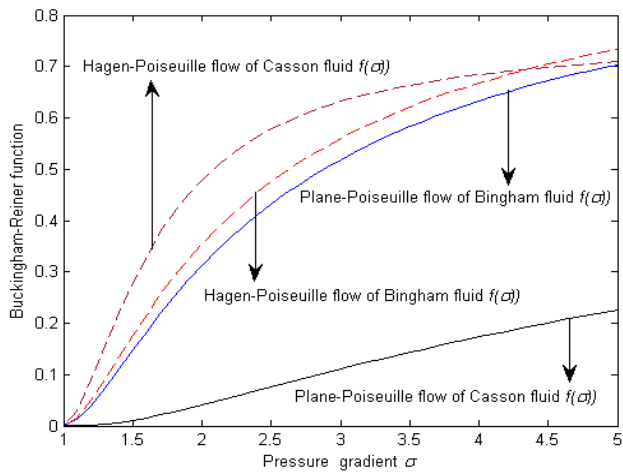
Fig. 3. Variation of Buckingham–Reiner function with pressure gradient for plane–Poiseuille flow and Hagen-Poiseuille flow of Casson and Bingham fluids.
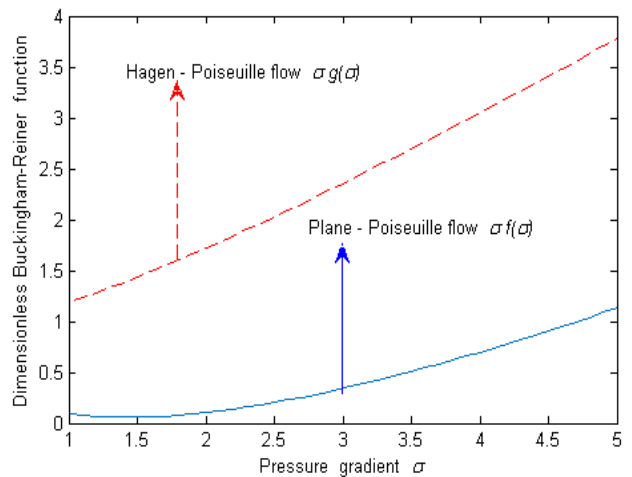

Fig. 4. Dimensionless Buckingham–Reiner function Vs. pressure gradient for plane–Poiseuille and Hagen Poiseuille flows.
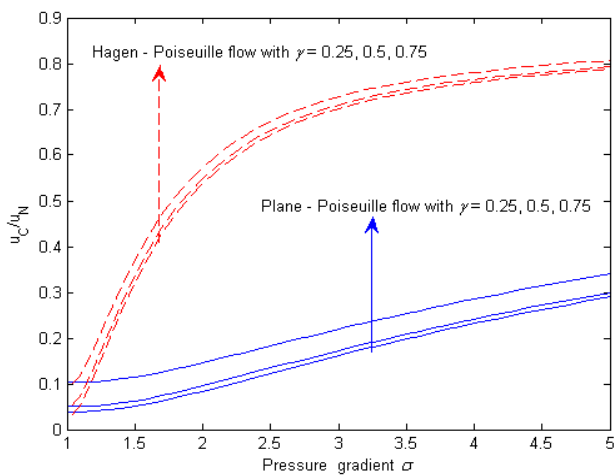

Fig. 5. Variation of mean velocity of Casson fluid with pressure gradient in the porous medium having multi-channel / tubes of different width/radii.
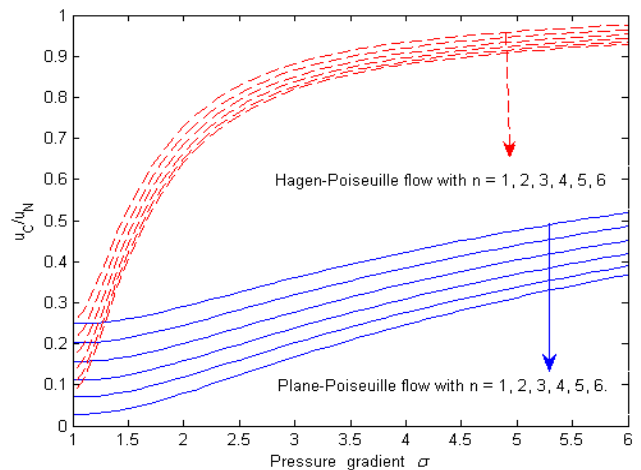

Fig. 6. Variation of mean velocity of Casson fluid with pressure gradient for flow in porous medium with several multi-channel/pipes with $\gamma_1 = 1, \gamma_2 = 0.9, \gamma_3 = 0.8, \gamma_4 = 0.7, \gamma_5 = 0.6$ and $\gamma_6 = 0.5$.

Fig. 7. Variation of the fluid's mean velocity with pressure gradient in the flow through porous medium with multi-channel of width/multi-pipe of radii $\gamma = 0.7, 0.75, 0.8, 0.85, 0.9, 0.95, 1$ when the pores in the flow medium are distributed in uniform distribution.
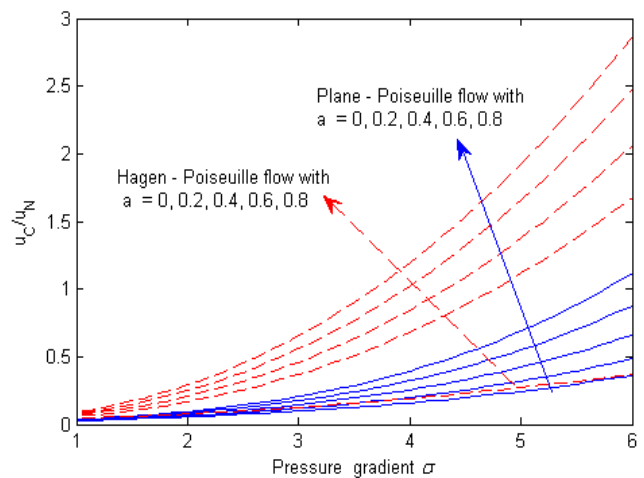

Fig. 8. Variation of mean velocity of Casson fluid with pressure gradient for flow in multi-channel/pipes with pores in the porous medium distributed in uniform distribution with $a = 0, 0.2, 0.4, 0.6, 0.8$.

It is well known that the constitutive equation of Bingham fluid is linear. Since the constitutive equation of Casson fluid is nonlinear, the Buckingham-Reiner functions of Casson fluid model for plane-Poiseuille flow (Eq. (9)) and Hagen-Poiseuille flow (Eq. (A2)) are highly nonlinear compared to those of Bingham fluid model (Eq. (6) and Eq. (48) in the paper of Nash and Rees [37] for plane-Poiseuille flow and Hagen-Poiseuille flow respectively). Hence, this nonlinearity leads to the abnormal variation in the Buckingham-Reiner functions of Casson and Bingham fluids between the plane-Poiseuille flow and Hagen-Poiseuille flow, which is transparent in Fig. 3.

The variation of dimensionless Buckingham-Reiner function $\sigma f(\sigma)$ (or $\sigma g(\sigma)$) with pressure gradient for plane-Poiseuille flow and Hagen-Poiseuille flow of Casson fluid through the porous medium is delineated in Fig. 4. It is seen that the dimensionless Buckingham-Reiner function increases almost linearly with the pressure gradient. When the pressure gradient σ is kept as constant, the Buckingham-Reiner function value is significantly higher in the Hagen-Poiseuille flow than in plane-Poiseuille flow. This means the cylindrical geometry of the flow medium enhances the volume flow over the rectangular geometry of the flow medium, and thus, the volume flow rate is significantly higher in Hagen-Poiseuille flow than in plane-Poiseuille flow. One can realize that the shape of the flow medium plays a vital role in enhancing the fluid's velocity.

3.2 Mean velocity in multi-channel/multi-pipe

Fig. 5 illustrates the variation in the mean velocity of Casson fluid with pressure gradient when it flows through the porous medium having multi-channel/multi-pipes of different width/radii. One can record that the mean velocity in plane-Poiseuille flow rises linearly when the pressure gradient increases, whereas in the Hagen–Poiseuille flow, it soars up when the pressure gradient increases from 1 to 2.5 and then it increases slowly when the pressure gradient increases from 2.5 to 5. It is also found that the mean velocity is significantly higher in the Hagen-Poiseuille flow than in plane-Poiseuille flow. i.e., the cylindrical geometry of the flow medium rises the fluid's mean velocity over the rectangular geometry of the flow medium.

The variation in the mean velocity of Casson fluid with the pressure gradient for flow in porous medium with several multi-channel/pipes with $n = 1,2,3,4,5,6$ $(\gamma_1 = 1, \gamma_2 = 0.9, \gamma_3 = 0.8, \gamma_4 = 0.7, \gamma_5 = 0.6, \gamma_6 = 0.5)$ is shown in Fig. 6. One may note that the mean velocity in plane–Poiseuille flow increases linearly with the rise of the pressure gradient σ, whereas in the case of Hagen–Poiseuille flow, it rises rapidly when the pressure gradient rises from 1 to 2.5, and then it increases slowly (almost constant) with the rise of the pressure gradient from 2.5 to 5. The reason behind this abnormal behavior of Casson fluid between the plane-Poiseuille flow and Hagen-Poiseuille flow is that in the case of Casson fluid flow in multi-pipes, the Buckingham-Reiner function (Eq. (A2)) and mean velocity (Eq. (A7)) are highly nonlinear compared to those of multi-channels fluid flow. One can also notice that the fluid's mean velocity is significantly higher in Hagen-Poiseuille flow than in plane-Poiseuille flow. It is also recorded that when the number of channels/pipes (n) in the flow medium increases, the fluid's mean velocity increases marginally in plane-Poiseuille flow, whereas in Hagen-Poiseuille flow, it increases very slightly.

3.3 Mean velocity in channels/pipes with uniform distribution of pores

Fig. 7 sketches the variation of the fluid's mean velocity with pressure gradient in the flow through a porous medium composed of multi-channel of widths/multi-pipe of radii $\gamma = 0.7, 0.75, 0.8, 0.85, 0.9, 0.95, 1$ when the pores in the flow medium are distributed in uniform distribution. It is seen that the fluid's mean velocity in plane-Poiseuille flow increases slowly when the pressure gradient rises; but in the Hagen-Poiseuille flow, it increases rapidly (nonlinearly) with the rise of pressure gradient from 1 to 2.5 and then it increases slowly with the further rise of pressure gradient from 2.5 to 5. Moreover, the fluid's mean velocity decreases slightly with the increase of the width of the channel/radius of the pipe. The variation of mean velocity with pressure gradient for flow in multi-channels/multi-pipes with pores distributed in uniform distribution for different values of the uniform distribution parameter a is rendered in Fig. 8. One can note that when the pressure gradient rises and rest of the parameters are treated as invariables, the mean velocity increases slowly (almost linearly) in plane-Poiseuille flow of Casson fluid, whereas it surges in the Hagen-Poiseuille flow of the fluid. It is also propounded that the fluid's mean velocity increases marginally with the increase of the uniform distribution parameter $'a'$ for the pores in the flow medium. For a given set of value of the parameters a and σ, the mean velocity is significantly higher in Hagen-Poiseuille flow than in plane-Poiseuille flow. From Figs. 7 and 8, one can spell out that the cylindrical geometry of the flow medium reduces the resistive forces to enhance the fluid's mean velocity over the rectangular geometry of the flow medium.

3.4 Mean velocity in channels/pipes with linear distribution of pores

The variation of mean velocity with pressure gradient for flow in multi-channel/multi-pipes with pores in these flow medium distributed in linear distribution of Type I for different width of multi-channels/radius of multi-pipes is plotted in Fig. 9. It is found that when the pressure gradient σ rises, the fluid's mean velocity increase very slowly in the plane-Poiseuille flow; whereas, in the Hagen-Poiseuille flow, it rises rapidly (nonlinearly). One can also notice that when the parameters σ and γ are treated as invariables, the fluid's mean velocity is significantly higher in Hagen-Poiseuille flow than in plane-Poiseuille flow. When the pressure gradient σ is held constant, the mean velocity raises marginally with the increase in the widths of the multi-channels/radii of the multi-pipes.

Fig. 10 delineates the variation in the mean velocity with pressure gradient in the plane-Poiseuille flow/Hagen-Poiseuille flow through porous medium with pores distributed in linear distribution of Type II for different values of channel width/pipe radius. One can notice that when the pressure gradient parameter σ increases, the mean velocity in plane-Poiseuille flow rises slowly; whereas in Hagen-Poiseuille flow, it linearly increases with the rise of pressure gradient σ from 1 to 3 and then it raises rapidly when pressure gradient increases further from 3 to 6. When the given pressure gradient σ is held constant, the mean velocity increases marginally with the rise of the channel width/pipe radius. It is noticed that when the flow parameters σ and γ are kept as constant, the mean velocity of the fluid is significantly higher in Hagen-Poiseuille flow than in plane-Poiseuille flow. From Figs. 9 and 10, one may record that the mean velocity of Casson fluid is significantly higher in the second type of linear distribution of pores than those recorded for the first type of linear distribution of pores. From Figs. (9) – (11), one can note that the mean velocity is considerably higher in circular geometry of the porous flow medium than in the rectangular geometry of the flow medium, meaning that the circular flow geometry enhances the fluid flow by overcoming from the resistive forces.
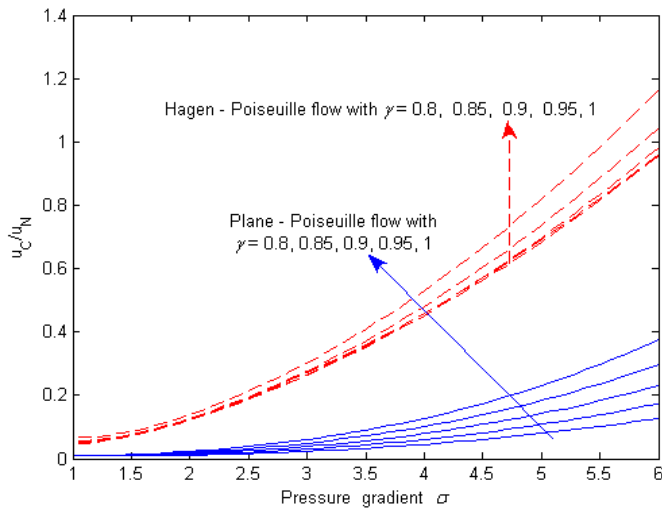
Fig. 9. Variation of mean velocity of Casson fluid with pressure gradient for flow in multi-channel/pipes with porous medium with pores distributed in linear distribution of Type I with γ = 0.8, 0.85, 0.9, 0.95, 1 .
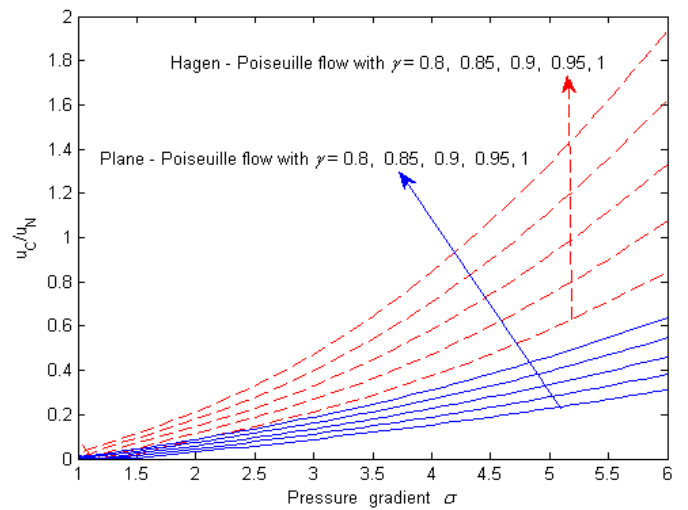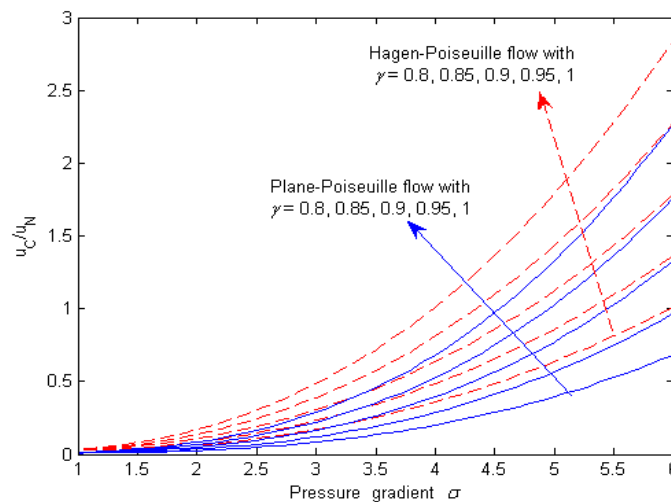

Fig. 10. Variation of mean velocity of Casson fluid with pressure gradient for flow in multi-channel/pipes with porous medium with pores distributed in linear distribution of Type II with γ = 0.8, 0.85, 0.9, 0.95, 1 .

Fig. 11. Variation of mean velocity of Casson fluid with pressure gradient for flow in multi-channel/pipes with porous medium with pores distributed in quadratic distribution with γ = 0.8, 0.85, 0.9, 0.95, 1 .

3.5 Mean velocity in channels/pipes with quadratic distribution of pores

Fig. 11 outlines the variation in the fluid's mean velocity with pressure gradient σ for plane-Poiseuille flow and Hagen-Poiseuille flow in a porous medium with pores distributed in quadratic distribution for various values of channel width and pipe radius. One can note that the mean velocity slowly increases with the rise of the pressure gradient σ from 1 to 4, and then it rises rapidly when the pressure gradient σ rises further from 4 to 6.In-plane-Poiseuille flow as well as Hagen-Poiseuille flow. The mean velocity raises considerably with the rise of the channel width and pipe radius when all the other parameters were held constant. One can also note that the fluid's mean velocity is considerably higher in Hagen-Poiseuille flow through porous medium than in plane-Poiseuille flow through the porous medium.

3.6 Porosity of the flow medium

Figs. 12 (i) – 12(iv) limn the variation in the porosity of the flow medium with the period of channels/pipes distribution H when the pores in the channels/pipes follow uniform distribution for different values of channel width/pipe radius and for the different values of the uniform distribution parameter 'a' such as (i)a = 0.8, (ii)a = 0.85, (iii)a = 0.9 and (iv)a = 0.95 . It is found that the porosity of the flow medium slumps with the rise of the period of the channels/pipes distribution parameter H from 1 to 2, and thereafter, it decreases very slowly with the further rise of the period of the channels/pipes H from 2 to 11. For a given period of the channels and pipes in the porous flow medium, the porosity increases marginally with the increase of the width of the rectangular channels and radius of the circular pipes. One may also observe that the porosity of the flow medium is higher in Hagen-Poiseuille flow than in plane-Poiseuille flow when the period H of the channels width/pipes radius lies between (i) 1 and 2 (when h = 0.7), (ii) 1 and 2.3 (when h = 0.8), (iii) 1 and 2.6 when h = 0.9 and (iv) 1 and 2.9 when h = 1.0. The porosity of the flow medium is higher in-plane-Poiseuille flow than in Hagen-Poiseuille flow when the period of the channels/pipes lies from the respective endpoint of each of the four-channel width/pipe radius mentioned above till H = 11 . From Figs. 12 (i) – 12 (iv), it is propounded that the porosity of the flow medium rises marginally with the rise of the parameter a of the uniform distribution.
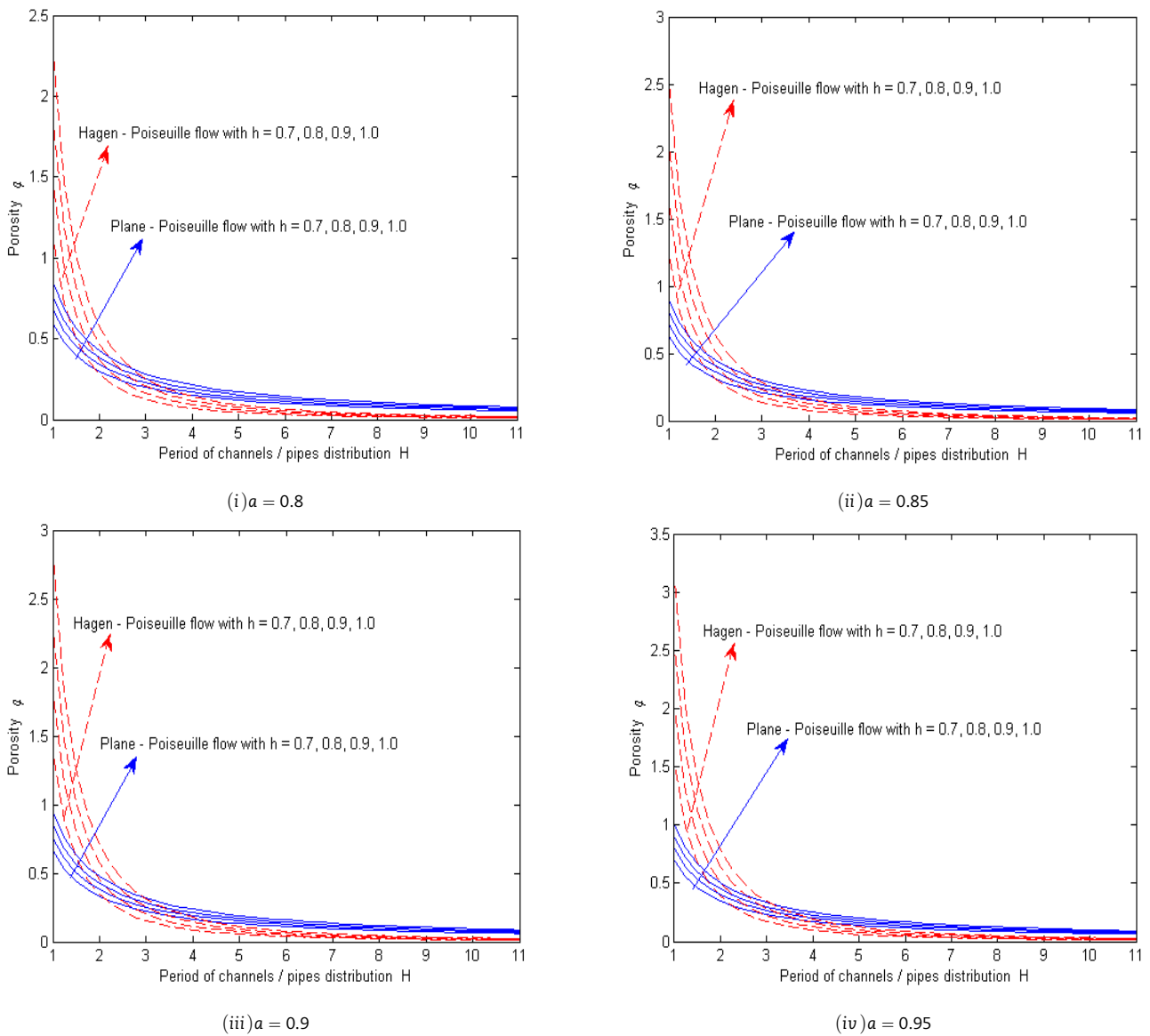
Fig. 12. Variation of porosity of the flow medium with the period of channels/pipes distribution when the pores in the channels/pipes follow uniform distribution for different values of width of channel/radius of pipe. $(i)a = 0.8$, $(ii)a = 0.85$, $(iii)a = 0.9$ and $(iv)a = 0.95$.
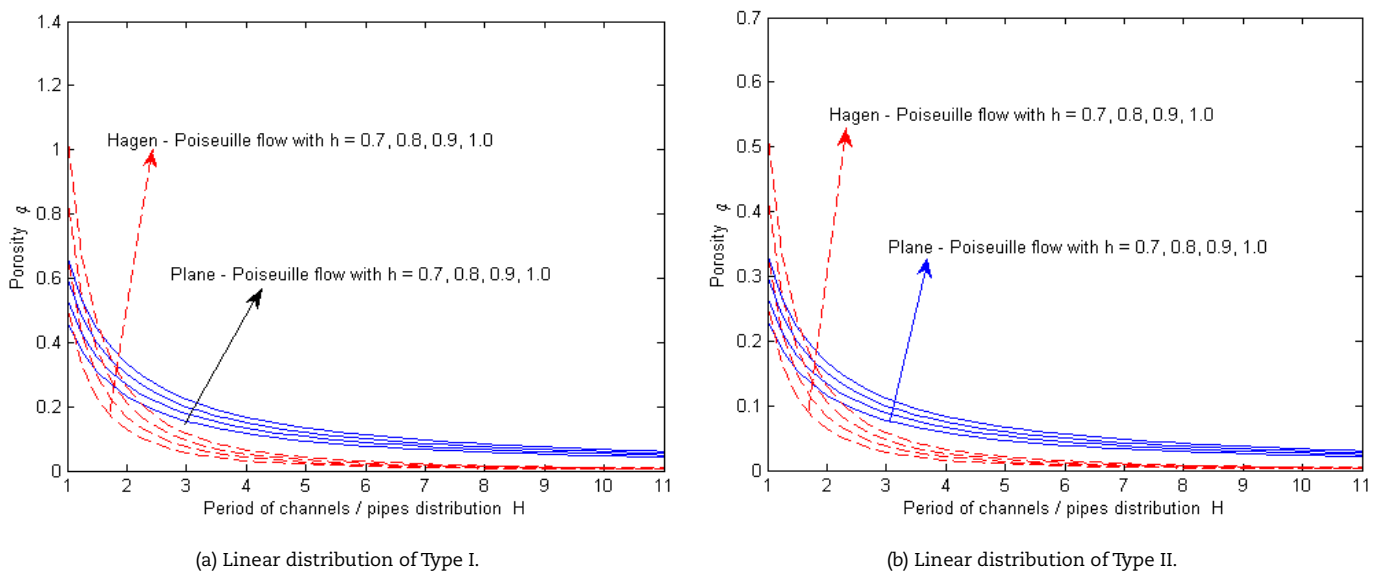

(a) Linear distribution of Type I.

(b) Linear distribution of Type II.

Fig. 13. Variation of porosity/permeability of the flow medium with the period of channels/pipes distribution when the pores in the channels/pipes follow the linear distribution of Type I and Type II for different values of width of channel/radius of pipe.
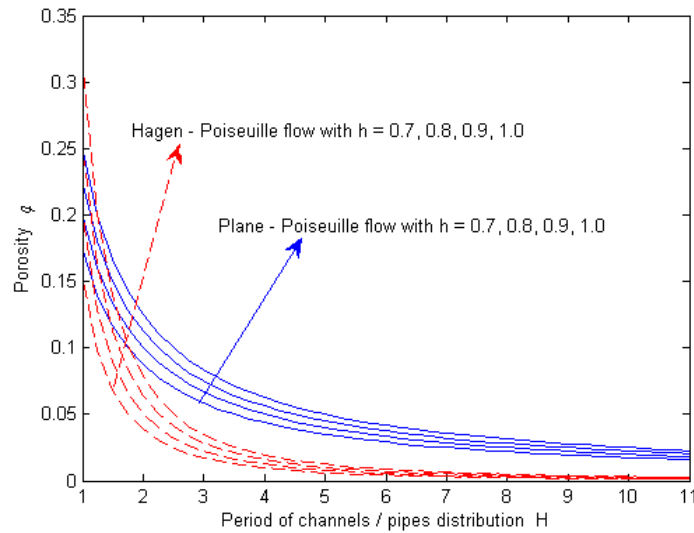
Fig. 14. Variation of porosity of the flow medium with the period of channels/pipes distribution when the pores in the channels/pipes follow quadratic distribution for different values of channel width/pipe radius.
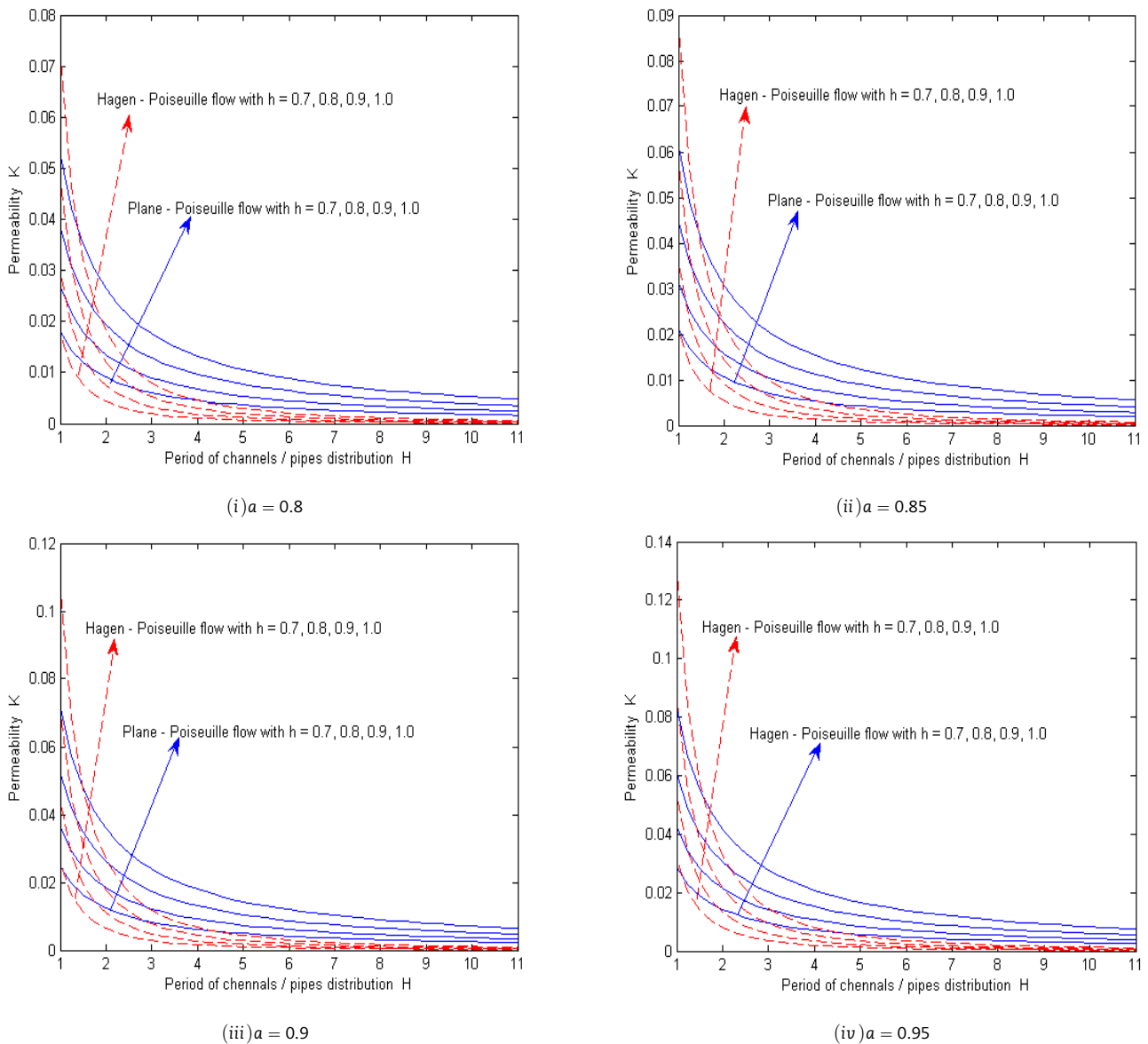

$(i)a = 0.8$

$(ii)a = 0.85$

$(iii)a = 0.9$

$(iv)a = 0.95$

Fig. 15. Variation of permeability of the flow medium with the period of channels/pipes distribution when the pores in the channels/pipes follow uniform distribution for different values of width of channel/radius of pipe. $(i)a = 0.8, (ii)a = 0.85, (iii)a = 0.9$ and $(iv)a = 0.95$.

The variations which are observed in Figs. 12 (i) to 12 (iv) for the porosity of the flow medium with respect to the period of channels and pipes parameter H and, channels width and pipe radius parameter h, are also observed from Figs. 13 (a), 13 (b) and (14) when the pores distribution in channels and pipes follow linear distribution of Type I, linear distribution of Type II and quadratic distribution respectively. From Figs. 13 (a) and 13 (b), one can find that the porosity of the flow medium is significantly higher when the pores in the medium of flow are distributed in the linear distribution of Type I than in the linear distribution of Type 2.

3.7 Permeability of the flow medium

Figs. 15 (i) – 15 (iv) delineates the variation of permeability of the flow medium with the period H of channels/pipes distribution when the pores in the channels/pipes follow uniform distribution for different values of width of channels/radius of pipes with $(i)a = 0.8$, $(ii)a = 0.85$, $(iii)a = 0.9$ and $(iv)a = 0.95$. It is clear that the flow medium's permeability decreases significantly with the rise of the period of channels and pipes from 1 to 2, and then it decreases very slowly when the period H of the channels and pipes increases from 2 to 11. One may also note that the permeability of the flow medium rise considerably with the rise of the channels width and pipe radius when all of the other parameters are treated as invariables. When the parameters H and h were held fixed, the permeability of the flow medium marginally rises with the raise of the parameter a of the uniform distribution. It is noted that the permeability in the flow medium is marginally higher for plane-Poiseuille flow than in the Hagen-Poiseuille flow.

The kind of variations which are observed in Figs. 15 (i) to 15 (iv) for the permeability of the flow medium with respect to the period of channels and pipes parameter H and, channels width and pipe radius parameter h, are also noticed from Figs. 16 (a), 16 (b) and Fig. 17, when the pores distribution in channels and pipes follow the linear distribution of type I, linear distribution of type II, and quadratic distribution, respectively. From Figs. 16 (a) and 16 (b), one can point out that the permeability of the flow medium is considerably higher when the pores in the flow medium are distributed in the linear distribution of Type I than in the linear distribution of Type II.
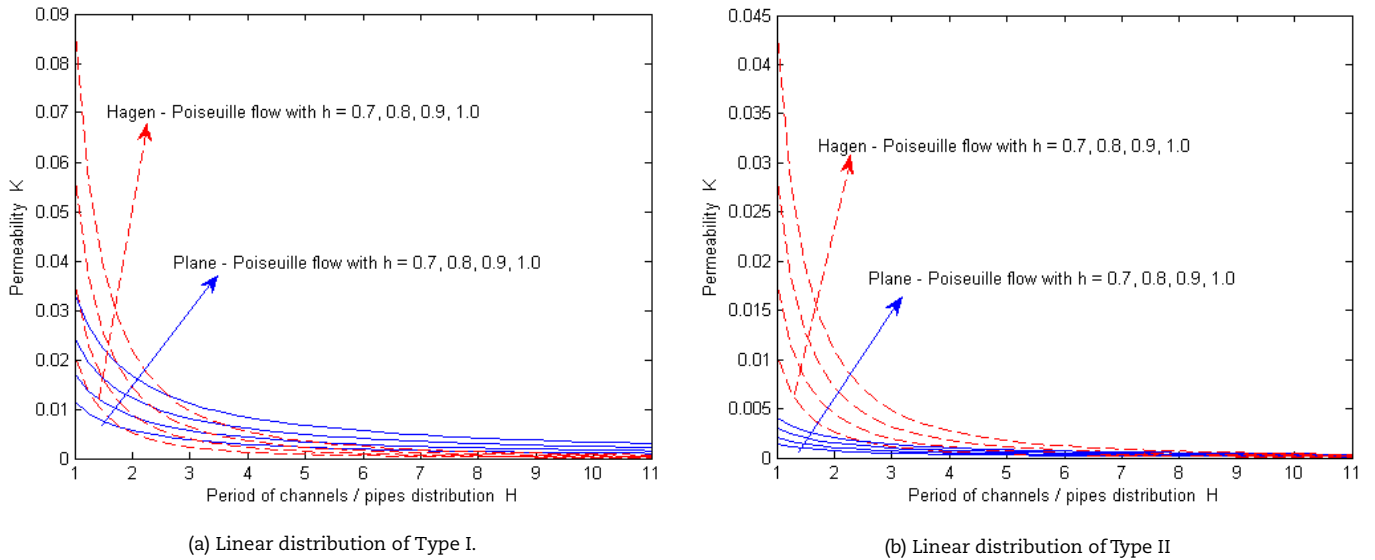

(a) Linear distribution of Type I.   (b) Linear distribution of Type II

Fig. 16. Variation of permeability of the flow medium with the period of channels/pipes distribution when the pores in the channels/pipes follow the linear distribution of Type I and II for different values of semi-width of channel/radius of pipe.
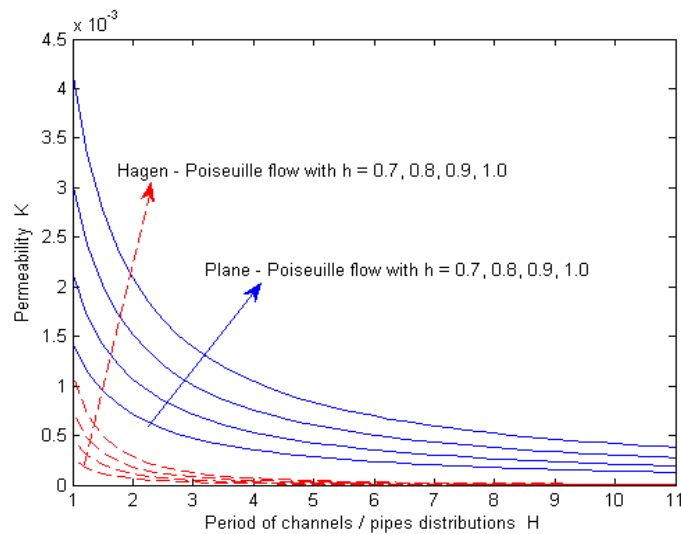

Fig. 17. Variation of permeability of the flow medium with the period of channels/pipes distribution when the pores in the channels/pipes follow quadratic distribution for different values of semi-width of channel/radius of pipe.

3.8 Discussion on the linear distributions of pores size

From Figs. 10(a), 10(b), 13(a), 13(b) 16 (a) and 16 (b), it is observed that the porosity and permeability of the flow medium are considerably higher when the pores in the flow medium are distributed in the linear distribution of Type I than in the linear distribution of Type II, and this behavior is revered for mean velocity. This is due to the fact that the gradient $d\psi/d\gamma$ of the Type I and Type II of the linear distribution pores are positive and negative respectively (i.e., the pore size increases with the channels widths ratio/pipes radii ratio parameter γ in Type I of linear distribution, while it decreases with γ in Type II of linear distribution). Thus, for a given value of γ, the pore size in Type I of linear distribution of pores is larger than that in Type II of linear distribution of pores, hence the porosity and permeability of fluid (amount of fluid observed by the pores) in Type I of linear distribution of pores are significantly higher than those in Type II of linear distribution of pores. Hence, the mean velocity of the fluid in the flow through channels/pipes in which the pores size distribution follows Type II of linear distribution of pores is significantly higher (almost double) than the fluid's mean velocity in channels/pipes in which the pores size distribution follows Type I of linear distribution of pores.

4. Conclusions

In this mathematical analysis, the influence of various flow parameters on the rheological measures was investigated in the plane-Poiseuille flow and Hagen-Poiseuille flow of Casson fluid through a porous medium consisting of (i) single-channel/pipe and (ii) multiple–channel/multiple-pipe when the pores in the multiple-channels/multiple-pipes are distributed in (i) uniform distribution, (ii) linear distribution of Type I, (iii) linear distribution of Type II and (iv) quadratic distribution. The main finding of this study are collated hereunder:

- When the pressure gradient rises, the Buckingham-Reiner function (flow rate) raises slowly in plane-Poiseuille flow, whereas in Hagen-Poiseuille flow, it rises rapidly.
- At a given level of pressure gradient, the Buckingham-Reiner function has markedly higher value in the Hagen-Poiseuille flow than in plane-Poiseuille flow.
- In all kinds of distribution of pores, the fluid's mean velocity and porosity of the flow medium are appreciably higher in Hagen-Poiseuille flow than in plane-Poiseuille flow, and this behavior is reversed for the permeability of the flow medium.
- With the rise of the pressure gradient, the mean velocity raises linearly in plane-Poiseuille flow; but in Hagen – Poiseuille flow, it soars up when the pressure gradient rises from 1 to 2.5 and then it increases slowly with the rise of pressure gradient from 2.5 to 5.
- The fluid's mean velocity, porosity, and permeability of the flow medium rises considerably with the increase of the channel width and pipe radius.
- The fluid's mean velocity, porosity, and permeability of the flow medium increase marginally with the rise of the uniform distribution parameter a.
- The porosity of the flow medium slumps with the rise of the period H of the channels and pipes distribution from 1 to 2, and it decreases very slowly with the further rise of the period of the channels and pipes H from 2 to 11.
- The porosity and permeability of the flow medium are considerably higher when the pores in the flow medium are distributed in the linear distribution of Type I than in the linear distribution of Type II, and this behavior is revered for mean velocity.

Given the results obtained in this study, it is hoped that the present mathematical analysis would provide a better understanding to the readers on the rheological characteristics of non-Newtonian fluid flow through porous media in which the distribution of pores follow different kinds of probability distribution. It is further believed that this study would motivate the readers to do further research in this field and also to produce more novel results.

Author Contributions

D.S. Sankar perceived the research problem, formulated it as a mathematical model and contributed to obtaining the analytical solutions, and also take part in developing MATLAB code for generating data for plotting the graphs and then analyzing the results. K.K. Viswanathan contributed to obtaining the expressions for rheological quantities and involved in generating the data for plotting the graphs through MATLAB programming and analyzed and validated the results. All the authors contributed to the manuscript preparation. All authors discussed the results, reviewed, and approved the final version of the manuscript.

Acknowledgment

Conflict of Interest

The authors declared no potential conflicts of interest with respect to the research, authorship, and publication of this article.

Funding

Data Availability Statements

The datasets generated and/or analyzed during the current study are available from the corresponding author on reasonable request.

Nomenclature

F	Darcy velocity u_c/u_N in plane-Poiseuille flow	a	Parameter associated with the uniform distribution
G	Darcy velocity u_c/u_N in Hagen-Poiseuille flow	f	Buckingham-Reiner law for plane-Poiseuille flow
H	Period of the pattern of channels/pipe	g	Buckingham-Reiner law for Hagen-Poiseuille flow
K	Permeability of the flow medium	h	Semi-width / radius of the channel/pipe
N	Number of channel/pipes	u_c	Axial velocity of Casson fluid
p	Pressure in the fluid flow through channel/pipe	u_N	Axial velocity of Newtonian fluid
Q	Volumetric flow rate in channel/pipe	r	Radial coordinate in polar coordinates
y	Vertical coordinate in Cartesian coordinates	x	Horizontal coordinate in Cartesian coordinates
z	Axial coordinate in polar coordinates		

Greek symbols

Ω	Negative of the pressure gradient	γ	Channel width/ pipe radius relative to h
μ	Dynamic viscosity	$\in$	Unyielded portion of the pipe/channel
σ	Dimensionless pressure gradient	τ	Shear stress
ϕ	Porosity of flow medium	τ_y	Yield stress

Subscript

C	Casson fluid	y	Yield stress
N	Newtonian fluid	pt	Pseudo-thresholds of stress

Appendix

Hagen-Poiseuille flow of Casson fluid

Let us consider the Hagen-Poiseuille flow of Casson fluid through a circular tube of uniform radius h. The rate of flow of Casson fluid in a single channel (analogous to that of Eq. (8)) is:

$$Q = 2\pi \int_0^h u \, dr = 2\left[\int_0^{\in h} r\, u_{pl}\, dr + \int_{\in h}^h r\, u\, dr\right] = \frac{\pi\Omega h^4}{8\mu} g(\sigma) = \frac{\pi\Omega h^3}{4\mu}\sigma g(\sigma), \tag{A1}$$

where

$$g(\sigma) = \begin{cases} 1 - \dfrac{8}{7\sqrt{|\sigma|}} + \dfrac{4}{3|\sigma|} - \dfrac{8}{3|\sigma|^{5/2}} + \dfrac{31}{21|\sigma|^4} & \text{if } |\sigma| > 1 \\ 0 & \text{if } |\sigma| > 1 \end{cases}. \tag{A2}$$

The function $g(\sigma)$ obtained in Eq. (A1) is the Buckingham-Reiner function (formula) for the Hagen-Poiseuille flow of Casson fluid. The Darcy velocity of Casson fluid u_c for one period of the pattern of tubes is obtained as below:

$$u_C = \frac{\phi\Omega h^2}{8\mu} g(\sigma) = \frac{\Omega K}{\mu} g(\sigma), \tag{A3}$$

where

$$\phi = \frac{\pi h^2}{H^2} \text{ and } K = \frac{\phi h^2}{8}, \tag{A4}$$

When $\sigma >> 1$ the normalized mean velocity $g(\sigma)$ reduces to the following quadratic form:

$$g(\sigma) = \frac{32}{3}(\sigma-1)^2 - \frac{89}{3}(\sigma-1)^3 + \ldots, \quad 0 < (\sigma-1) << 1 \tag{A5}$$

For a significantly large value of σ $(\sigma >> 1)$, Eq. (A2) yields the three-term approximation to the induced flow as given in Eq. (A6).

$$\sigma g(\sigma) \approx \sigma - \frac{8}{7}\sqrt{\sigma} + \frac{4}{3}. \tag{A6}$$

For the porous medium, which has multi-tubes of radii $\gamma_i h$, $i = 1, 2, \ldots, N$, the Darcy velocity of Casson fluid in relation to Newtonian fluid, porosity, and permeability of the flow medium are given by Eqs. (A7) – (A9), respectively.

$$u_C/u_N = G(\sigma) = \left[\sum_{i=1}^N \gamma_i^4 g(\gamma_i\sigma) \middle/ \sum_{i=1}^N \gamma_i^4\right]. \tag{A7}$$

$$\phi = \left(\pi h^2/H^2\right)\sum_{i=1}^N \gamma_i^2 \tag{A8}$$

$$K = \left(\phi h^2 / 8\right)\left[\sum_{i=1}^{N} \gamma_i^4 \middle/ \sum_{i=1}^{N} \gamma_i^2\right]. \tag{A9}$$

The pseudo-threshold σ for the porous medium with N channels per period is given below:

$$\sigma_{pt} = 4\sum_{i=1}^{N} \gamma_i^3 \middle/ 3\sum_{i=1}^{N} \gamma_i^4. \tag{A10}$$

When probability density functions $\psi(\gamma)$ are used to describe the distribution of radius of circular tubes in a porous medium, then the Darcy velocity of the flow, porosity, and permeability of the flow medium are defined by Eqs. (A11) – (A13), respectively [37]:

$$F(\sigma) = \frac{u_C}{u_N} = \int_0^{\infty} \gamma^4 \psi(\gamma) g(\gamma\sigma) d\gamma \middle/ \int_0^{\infty} \gamma^4 \psi(\gamma) d\gamma, \tag{A11}$$

$$\phi = \left(\pi h^2 / H^2\right) \int_0^{\infty} \gamma^2 \psi(\gamma) d\gamma, \tag{A12}$$

$$F(\sigma) = \left(\phi h^2 / 8\right) \int_0^{\infty} \gamma^4 \psi(\gamma) d\gamma \middle/ \int_0^{\infty} \gamma^2 \psi(\gamma) d\gamma, \tag{A13}$$

(a)   Uniform distribution of pores

When the pores of circular tubes are uniformly distributed (as given in Eq. (28)), the expression for the Darcy velocity of the flow, porosity, and permeability of the flow medium is obtained as Eqs. (A14) – (A16), respectively:

$$G(\sigma) = \begin{cases} 0 & \text{if } 0 \le \sigma < 1 \\ \dfrac{63\sigma^5 - 80\sigma^{9/5} + 105\sigma^4 - 168\sigma^{5/2} - 465\sigma + 322}{63\sigma^5\left(1 - a^5\right)} & \text{if } 1 \le \sigma \le 1/a \\ 1 - \dfrac{80\left(1 - a^{9/2}\right)}{63\sqrt{\sigma}\left(1 - a^5\right)} + \dfrac{5\left(1 + a + a^2 + a^3\right)}{3\sigma\left(1 + a + a^2 + a^3 + a^4\right)} - \dfrac{8\left(1 - a^{5/2}\right)}{3\sigma^{5/2}\left(1 - a^5\right)} + \dfrac{155}{21\sigma^4\left(1 + a + a^2 + a^3 + a^4\right)} & \text{if } \sigma > \dfrac{1}{a} \end{cases} \tag{A14}$$

$$\phi = \left(\frac{\pi h^2}{H^2}\right)\frac{\left(1 + a + a^2\right)}{3}, \tag{A15}$$

$$K = \left(\frac{\phi h^2}{8}\right)\frac{\left(1 + a + a^2 + a^3 + a^4\right)}{5\left(1 + a + a^2\right)}. \tag{A16}$$

(b) Linear distribution of pores

For the first kind of linear distribution (given in Eq. (33)) of the pores in the circular tube, the expressions for Darcy velocity, porosity, and permeability are obtained as in Eqs. (A17) – (A19), respectively.

$$G(\sigma) = \begin{cases} 0 & \text{if } 0 \le \sigma \le 1 \\ \dfrac{385\sigma^6 - 480\sigma^{11/2} + 616\sigma^5 - 880\sigma^{7/2} + 3410\sigma - 3051}{385\sigma^6} & \text{if } \sigma > 1 \end{cases}, \tag{A17}$$

$$\phi = \frac{1}{2}\left(\frac{\pi h^2}{H^2}\right), \tag{A18}$$

$$K = \frac{2}{3}\left(\frac{\phi h^2}{8}\right). \tag{A19}$$

For the second kind of linear distribution (defined in Eq. (34)) of pores in the circular tube, the expressions for Darcy velocity, porosity, and permeability simplify to Eqs. (A20) – (A22).

$$G(\sigma) = \begin{cases} 0 & \text{if } 0 \le \sigma \le 1 \\ \dfrac{3\left(231\sigma^6 - 320\sigma^{11/2} + 462\sigma^5 - 1056\sigma^{7/2} + 5115\sigma^2 - 8470\sigma + 4038\right)}{462\sigma^6} & \text{if } \sigma > 1 \end{cases} \tag{A20}$$

$$\phi = \frac{\pi h^2}{6H^2}, \tag{A21}$$

$$K = \frac{2}{5}\left(\frac{\phi h^2}{8}\right). \tag{A22}$$

(c)   Quadratic distribution

When the pattern of the pores of the flow region is represented by quadratic distribution (defined in Eq. (41)), the expressions for Darcy velocity, porosity, and permeability of the flow medium simplifies to Eqs. (A23) – (A25).

$$G(\sigma) = \begin{cases} 0 & \text{if } 0 \leq \sigma \leq 1 \\ \dfrac{429\sigma^7 - 640\sigma^{13/2} + 1001\sigma^6 - 3050\sigma^{9/2} + 22165\sigma^3 - 55055\sigma^2 + 52494\sigma - 17343}{429\sigma^7} & \text{if } \sigma > 1 \end{cases} \tag{A23}$$

$$\phi = \frac{1}{10}\left(\frac{\pi h^2}{H^2}\right), \tag{A24}$$

$$K = \frac{1}{35}\left(\frac{\phi h^2}{8}\right). \tag{A25}$$

References

[1] Moller, B. P., Fall, A., Chikkadi, Y., Deres, D., Bonn, D., An attempt to categorize yield stress fluid behaviour, *Philosophical Transactions of Royal Society A*, 367, 2009, 5139 – 5155.
[2] Zhu, H., Kim, Y. D., Kee, D. D., Non-Newtonian fluids with yield stress, *Journal of Non-Newtonian Fluid Mechanics*, 129, 2015, 177 – 181.
[3] Coussot, P., Yield stress fluid flows: a review of experimental data, *Journal of Non-Newtonian Fluid Mechanics*, 211, 2014, 31 – 49.
[4] Papanastasiou, T. C., Flows of materials with yield stress, *Journal of Rheology*, 31, 1987, 385–404.
[5] Moller, P. C. F., Fall, A., Bonn, D., Origin of apparent viscosity in yield stress fluids below yielding, *EPL*, 87, 2009, 38004.
[6] Scott Blair, G. W., An Equation for the Flow of Blood, Plasma, and Serum through Glass capillaries, *Nature*, 183, 1959, 613–614.
[7] Balmforth, N. J., Frigaard, I. A., Ovarlez, G., Yielding to stress: recent developments in viscoplastic fluid mechanics, *Annual Reviews of Fluid Mechanics*, 46, 2014, 121–146.
[8] Charm, S C., Kurland, G S., Viscometry of human blood for shear rates of 0–100,000sec−1, *Nature*, 206, 1965, 617–618.
[9] Bingham, E. C., *Fluidity and Plasticity*, McGraw-Hill, New York, 1922.
[10] Harris J., Comments on "The flow of non-Newtonian fluids under a varying pressure gradient", *Nature*, 226, 1970, 848–849.
[11] Mitsoulis, E., Abdali, S. S., Flow simulation of Herschel–Bulkley fluids through extrusion dies, *Canadian Journal of Chemical Engineering,* 71, 1993, 147–160.
[12] Sankar, D. S., Two-phase non-linear model for blood flow in asymmetric and axisymmetric stenosed arteries, *International Journal of Non-Linear Mechanics*, 46, 2011, 296 – 305.
[13] Tu, C., Deville, M., Pulsatile flow of non-Newtonian fluids through arterial stenosis, *Journal of Biomechanics,* 29, 1996, 899-908.
[14] Venkatesan, J., Sankar, D. S., Hemalatha, K., Yazariah, Y., Mathematical analysis of Casson fluid model for blood rheology in stenosed narrow arteries, *Journal of Applied Mathematics*, 2013, Article ID: 583809.
[15] Chaturani, P., Ponnalagar Samy, R., Pulsatile flow of Casson's fluid through stenosed arteries with applications to blood flow, *Biorheology*, 23, 1986, 499–511.
[16] Nagarani, P., Sarojamma, G., Effect of body acceleration on pulsatile flow of Casson fluid through a mild stenosed artery, *Korea–Australia Rheology Journal*, 20, 2008, 189–96.
[17] Dullien, F. A. L., *Porous Media – Fluid Transport and pore structure*, Second Edition., Academic Press, 1992.
[18] Balhoff, M. T., Rivera, D. S., Kwok, A., Mehmani, Y., Prodanovic, M., Numerical algorithms for network modeling of yield stress and other non-Newtonian fluids in porous media, *Transport in Porous Media,* 93, 2012, 363–379.
[19] Bleyer, J., Coussot, P., Breakage of non-Newtonian character in flow through porous medium: evidence from numerical simulation, *Physical Review E -American Physical Society*, 89, 2014, 063018.
[20] Chevalier, T., Chevalier, C., Clain, X., Dupla, J. C., Canou, J., Rodts, S., Cousso, P., Darcy's law for yield stress fluid flowing through a porous medium, *Journal of Non-Newtonian Fluid Mechanics*, 195, 2013, 57–66.
[21] Chen, M., Rossen, W., Yortsos, Y. C., The flow and displacement in porous media of fluids with yield stress, *Chemical Engineering Science*, 60, 2005, 4183–4202.
[22] Darcy, H., *Les fontaines publiques de la ville de Dijon*, Victor Dalmont, Paris,1856.
[23] Oukhlef, A., Champmartin, S., Ambari, A., Yield stress fluids method to determine the pore size distribution of a porous medium, *Journal of Non-Newtonian Fluid Mechanics*, 204, 2014, 87 - 93.
[24] Ho, C. K., Webb, S.W., *Theory and Application of Transport in Porous Media, Gas Transport*, Springer 2006.
[25] Wulff, M., Pore size determination by thermoporometry using acetonitrile, *Thermochimica Acta,* 419, 2004, 291–294.
[26] Brun, M., Lallemand, A., Quinson, J. F., Eyraud, C., A new method for the simultaneous determination of the size and the shape of pores: the thermoporometry, *Thermochimia Acta*, 21, 1977, 59–88.
[27] Heinemann, Z. E., *Fluid flow in porous media*, Textbook Ser. 1 2003.
[28] Barrett, E. P., Joyner, L. G., Halenda, P. P., The determination of pore volume and area distributions in porous substance, computations from nitrogen isotherms, *Journal of American Chemical Society*, 73, 1951, 373 – 380.
[29] Bingham, E. C., An investigation of the laws of plastic flow, *US Bureau of Standards Bulletin*, 13, 1996, 309–353.
[30] Reiner, M., Ueber die Strömung einer elastischen Flüssigkeit durch eine Kapillare. Beitrag zur Theorie Viskositätsmessungen, *Colloid and Polymer Science*, 39, 1926, 80–87.
[31] Pascal, H., Nonsteady flow of non-Newtonian fluids through a porous medium, *International Journal of Engineering Science*, 21, 1983, 199–210.
[32] Sabiri, N. E., Comiti, J., Pressure drop in non-Newtonian purely viscous fluid flow through porous media, *Chemical Engineering Science*, 50, 1995, 1193–1201.
[33] Daprà, I., Scarpi, G., Start-up of channel-flow of a Bingham fluid initially at rest, *Rendiconti Lincei Matematica e Applicazioni*, 9, 2004, 125–135.
[34] Daprà, I., Scarpi, G., Start-up flow of a Bingham fluid in a pipe, *Meccanica*, 40, 2005, 49–63.
[35] Chevalier, T., Talon, L., Moving line model and avalanche statistics of Bingham fluid flow in porous media, *European Physical Journal E*, 38, 2015, 76 - 81.
[36] Chevalier, T., Rodts, S., Chateau, X., Chevalier, C., Coussot, P., Breaking of non-Newtonian character in flows through porous medium, *Physical Reviews Journal E*, 89, 2014, 023002.

[37] Nash, S., Andrew, D., Rees, S., The effect of microstructure on models for the flow of Bingham fluid in porous media: One-dimensional flows, *Transport in Porous Media,* 116, 2017, 1073 – 1092.

[38] Lopez, X., Valvatne, P. H., Blunt, M. J., Predictive network modeling of single-phase non-Newtonian flow in porous media, *Journal of Colloid Interface Science,* 264, 2003, 256–265.

[39] Al-Fariss, T., Pinder, K. L., Flow-through porous media of a shear-thinning liquid with a yield stress, *Canadian Journal of Chemical Engineering,* 65, 1987, 391–405.

[40] Purcell, W. R., Capillary pressures—their measurement using mercury and the calculation of permeability therefrom, *Petroleum Transactions AIME,* 186, 1949, 39–48.

ORCID iD

D.S. Sankar https://orcid.org/0000-0002-2039-5922
K.K. Viswanathan https://orcid.org/0000-0003-4470-4774

Publisher's Note Shahid Chamran University of Ahvaz remains neutral with regard to jurisdictional claims in published maps and institutional affiliations.